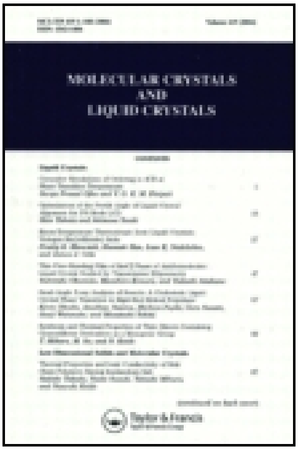

Molecular Crystals and Liquid Crystals

Publication details, including instructions for authors and subscription information:
http://www.tandfonline.com/loi/gmcl16

Helical Alignment of Field-Dependent Structures in Cholesteric Phase

H. Asai [a] , M. Terasaki [a] , T. Hasegawa [a] & S. Kurita [a]

[a] Department of Electrical Engineering, Faculty of Engineering, Keio University, Hiyoshi, Kohoku, Yokohama, Japan, 223

Version of record first published: 14 Oct 2011.

To cite this article: H. Asai , M. Terasaki , T. Hasegawa & S. Kurita (1982): Helical Alignment of Field-Dependent Structures in Cholesteric Phase, Molecular Crystals and Liquid Crystals, 84:1, 285-307

To link to this article: http://dx.doi.org/10.1080/00268948208072148

Mol. Cryst. Liq. Cryst., 1982, Vol. 84, pp. 285–307
0026-8941/82/8401-0285 $06.50/0

Helical Alignment of Field-Dependent Structures in Cholesteric Phase†

H. ASAI, M. TERASAKI, T. HASEGAWA and S. KURITA

Department of Electrical Engineering, Faculty of Engineering, Keio University, Hiyoshi, Kohoku, Yokohama, Japan, 223

(*Received August 15, 1980; in final form October 12, 1981*)

The field-dependent structure in cholesteric phase has been investigated using several experiments. We have selected the azimuthal angle of a molecular layer ϕ and tilt angle in the direction of helical axis θ as the components of static deformation, and defined a new parameter as a degree of helical alignment by numerical value, $Q \equiv 2\{1 - [\langle \sin^2 \phi \rangle]\}[\langle \cos^2 \theta \rangle] \equiv 2(1 - r)q$.

For perfectly helical alignment, $Q = 1$, while for nematic state with helical alignment disappearing, $Q = 0$.

The relation between these parameters and experimentally determined quantities, typical Q, and the method to measure the orientational order S in cholesterics using Q, were discussed.

1 INTRODUCTION

The cholesteric phase has been found to be isostructual with nematic phase, which has both helical structure and nematic alignment in layers. Responses of the helical structure to an external condition are useful to physical aspects and the application to displays. The phenomena are due to the fact that the helical energy has the order of external field energy and surface interaction. Therefore, the helical structure tends to be deformed easily by these conditions. Consequently, in order to show the deformation, we should make the various conditions clear; cell thickness, surface treatment, pitch length, external field etc. But the trouble is that this process brought some obscure points and misunderstandings of papers.

For the nematic phase the order parameter is defined to show molecular orientational order, and its thermodynamic state can be evaluated numeri-

---

†Presented at the VIIIth International Liquid Crystal Conference, Kyoto, Japan, June 30–July 4, 1980.

cally.[1,2] Although some studies have been attempted to measure the orientational order in cholesteric phase using nematic order parameter,[3,4] it didn't give any information about its helical alignment.

We have studied the helical structures with static deformation caused by some external conditions. The data led to the definition of a new parameter "helical order parameter" Q representing the degree of helical alignment. We define the perfectly helical structure as $Q = 1$, and the nematic state with helical alignment disappeared as $Q = 0$. Thus, the helical parameter represents directly the physical state of cholesteric phase.

The experiments were performed on cholesteric-nematic liquid crystal mixtures with positive dielectric anisotropy. The process of structure change from initial state of cholesteric phase to electric field-induced nematic state[5,6] was observed. The homeotropic treatment which accelerates the phase change, and parallel treatment which disturbs it were used as the treatment of plates. On the basis of the results, and selecting the important components of deformation, we defined the helical order parameter as a function of them.

We discussed the relationship between this parameter and certain experimental quantities, and its usefulness.

2 EXPERIMENTAL PROCEDURES

The liquid crystals used here were mixtures of *p*-methoxy-benzilidene-*p'*-butylaniline (MBBA), *p*-ethoxybenzilidene-*p'*-butylaniline (EBBA), *p*-biphenyl-*p'*-cyanoaniline (BPCA), and cholesteryl nonanoate (CN) at weight ratio of $46:(34 - x):20:x$, where x varied from 0 to 5 wt.%. Each cholesteric mixture has a initial pitch p_0 of $11.8/x$ μm, a positive dielectric anisotropy ϵ_a of about +4.3 at 1 kHz AC, and a clearing point of about 56°C. It was loaded between two glass plates coated with transparent SnO_2 electrodes.

The sample thickness was determined by Mylar spacers of 20 μm. Homeotropic boundary condition was obtained by treating the surfaces of the electrodes with surfactant of chromic complex compound. Parallel boundary condition was achieved by rubbing them after treating similarly with polyamide resin. The rubbing direction of plate was changed according to the initial pitch p_0, so that the helical structure might not be distorted.

The microscopic observation of initial pitch and structure was done by the wedge shaped cell.

The deformations of helical structure in the presence of electric field at 500 Hz AC were investigated using several techniques such as dielectric measurements, transmission measurements, light scattering analysis and microscopic observations. Light source was He—Ne laser ($\lambda = 632.8$ nm) and sample temperature was stabilized at 19 ± 1°C.

3 RESULTS

The relationship between helical force in cholesterics and surface interaction can be expressed by the relative ratio of intrinsic pitch p to cell thickness d, d/p, which corresponds to the characteristic constant of the sample.

Homeotropic boundary condition sample

Initial state of sample is remarkably influenced by d/p. In the region of $d/p < 1$, boundary-induced homeotropic nematic alignment was observed. In the region of $d/p > 1$, however, microscopic observation shows periodic lines (Figure 1a), which indicate helical structure. When the d/p increased, microscopic patterns become included and turned into the eddy state (Figure 1e).

Figure 1 shows the sequential microscopic photographs for two samples under an electric field. [(Figure 1a–d) are the case of $d/p = 1.18$, and (e–h) are the case of $d/p = 3.38$.] And Figure 2 shows the dependence of the relative capacitance change $\Delta C/C_0$ and transmission change $\Delta T/T_0$ for the same samples. T_0 and C_0 are respectively the transmission and the capacitance of the initial structure. $\Delta C = C - C_0$ is the capacitance change and ΔT is the transmission change caused by field-induced structure change.

The distance between the periodic lines corresponds to a half pitch of helical structure whose axis is parallel to the plate. When the electric field increased, the dark homeotropic part (because observations were performed through clossed polarizers) increases (Figure 1b–d). In this case, the deformation is due to the azimuthal angle change of molecular layer. Therefore, $\Delta C/C_0$ and $\Delta T/T_0$ in Figure 2a increase gradually.

In the case of $d/p = 3.38$ sample, the winding of eddy state (Figure 1e–f) involves the rapid changes in $\Delta T/T_0$ and $\Delta C/C_0$ (Figure 2b). The light scattering profile from (*f*) and (*g*) pattern presents diffraction pattern as shown in Figure 4a.

Therefore, we conclude that helical axis rotates to the focal conic state. When $\Delta T/T_0$ and $\Delta C/C_0$ become constant, the structure changes into homeotropic nematic.

Parallel boundary condition sample

Initial structure was grandjean state for all samples. Figure 3 shows the microscopic observation for the sample under an electric field (with crossed polarizers).

As electric field increased, the microscopic patterns change; grid-like pattern—periodic lines (random orientation)—periodic lines (orientation)—color region (Figure 3a–d).

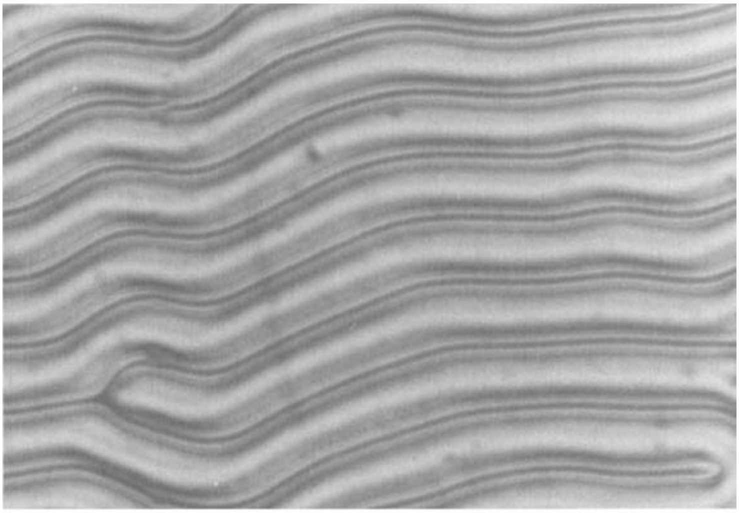

(a)

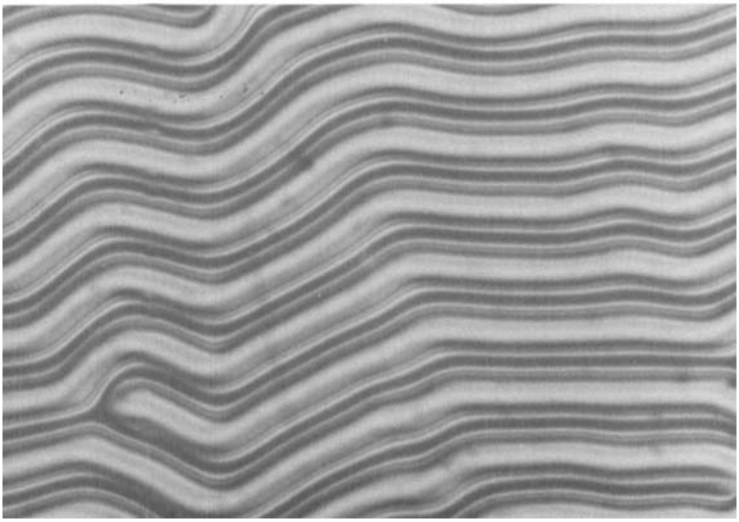

(b)

FIGURE 1 Photographs of the microscopic patterns from homeotropic boundary condition samples: crossed polarizers; (a–d) $d/p = 1.18$, (e–h) $d/p = 3.38$—(a) $E = 0$ (b) $E = 34.5$ V/mm (c) $E = 57.5$ V/mm (d) $E = 66.0$ V/mm (e) $E = 0$ (f) $E = 250$ V/mm (g) $E = 420$ V/mm (h) $E = 480$ V/mm.

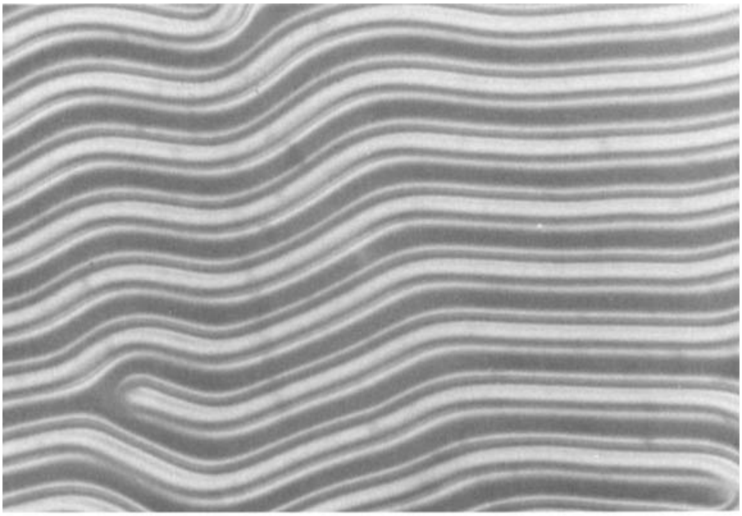

(c)

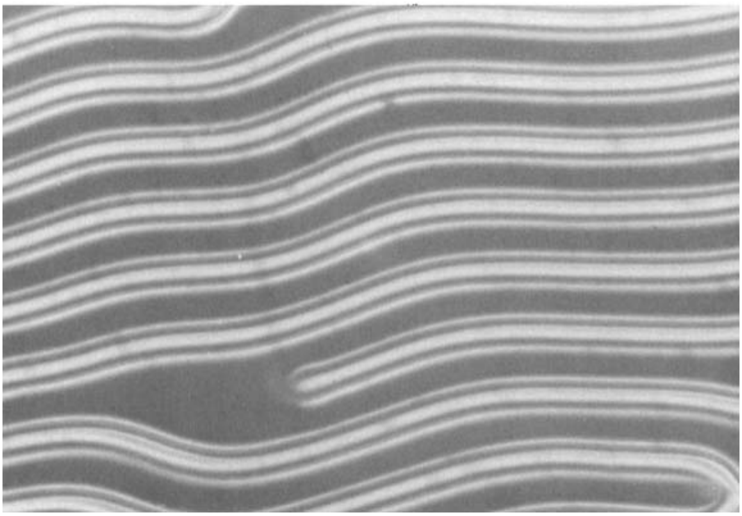

(d)

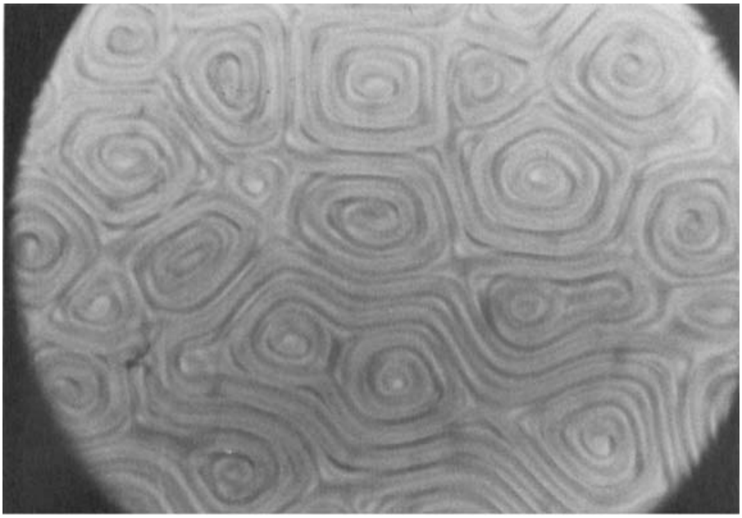

(e)

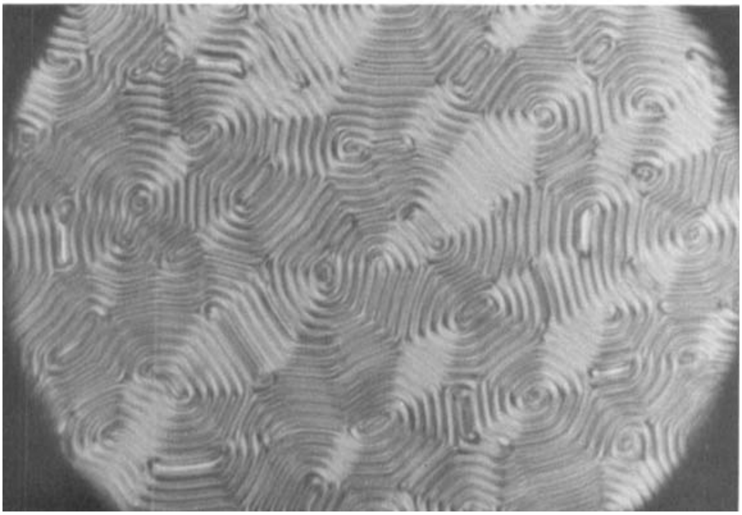

(f)

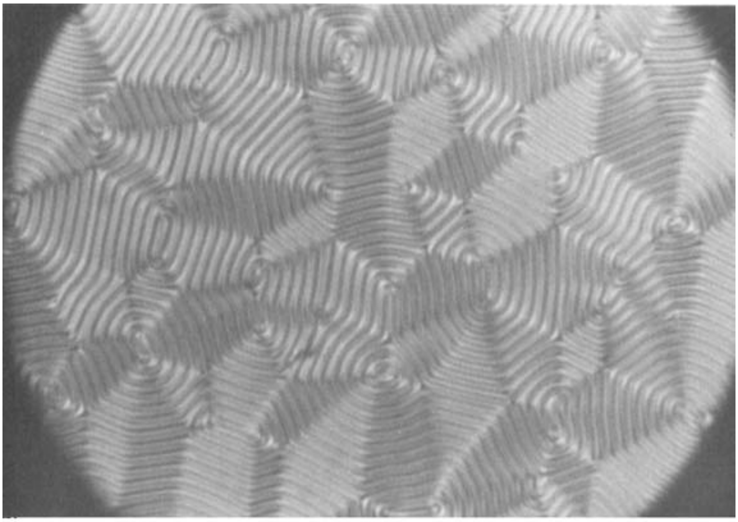

(g)

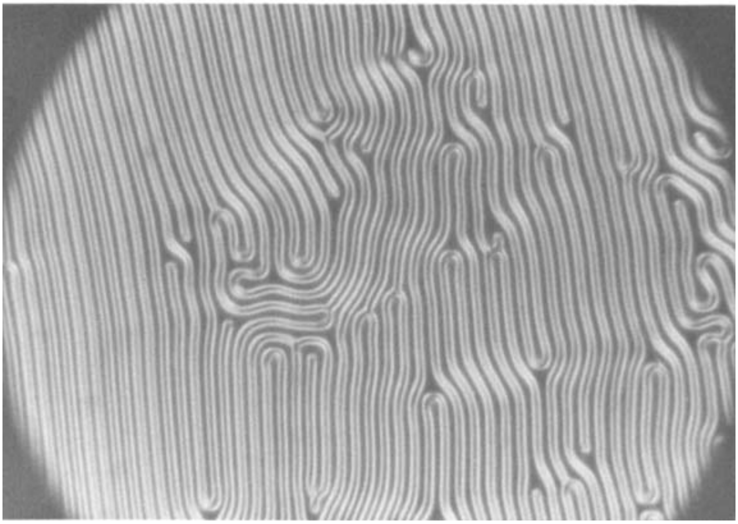

(h)

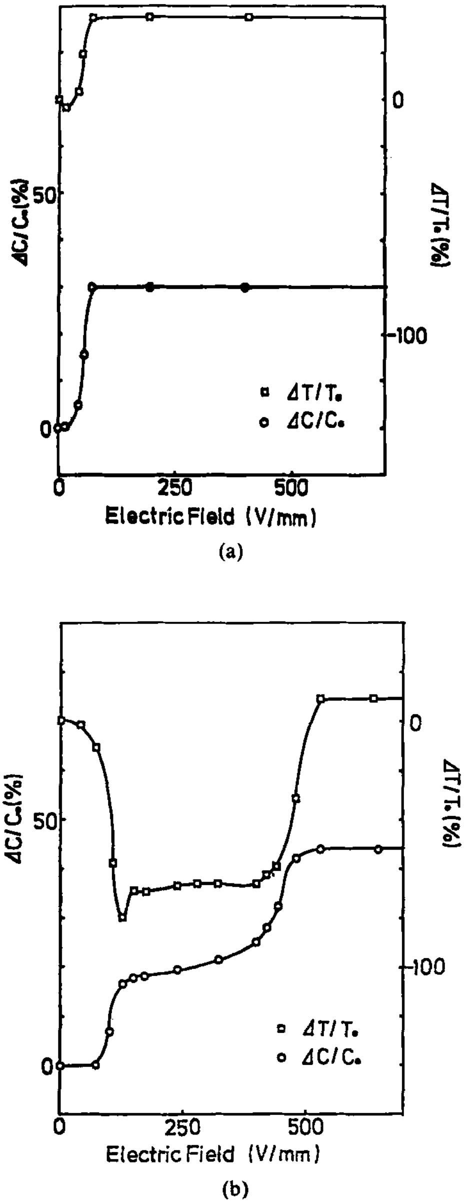

FIGURE 2 Relative capacitance change and relative transmission change vs. applied electric field: homeotropic boundary condition sample was used: subscript 0 implies zero field. (a) $d/p = 1.18$ (b) $d/p = 3.38$.

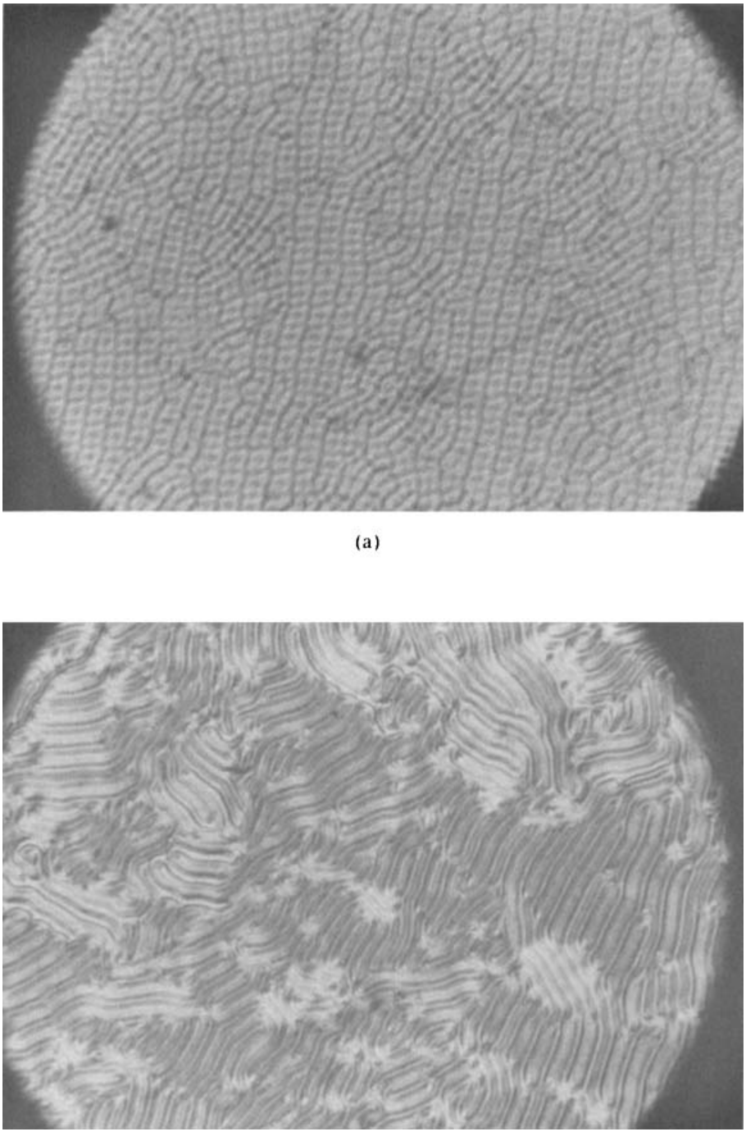

(a)

(b)

FIGURE 3 Photographs of the microscopic patterns from parallel boundary condition samples: crossed polarizers; (a, b) $d/p = 3.38$, (c, d) $d/p = 1.01$—(a) $E = 247$ V/mm, grid pattern (b) $E = 248$ V/mm, periodic lines (random orientation) (c) $E = 118$ V/mm, periodic lines (orientation) (d) $E = 147$ V/mm, color region.

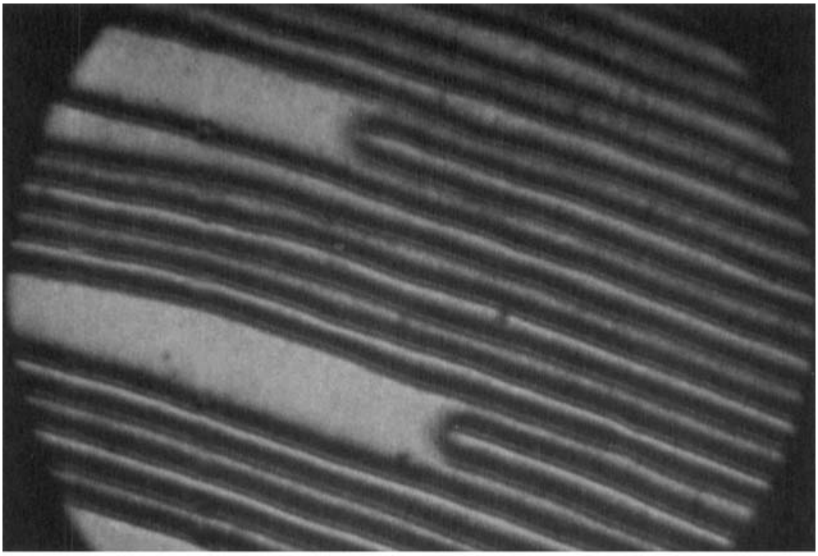

(c)

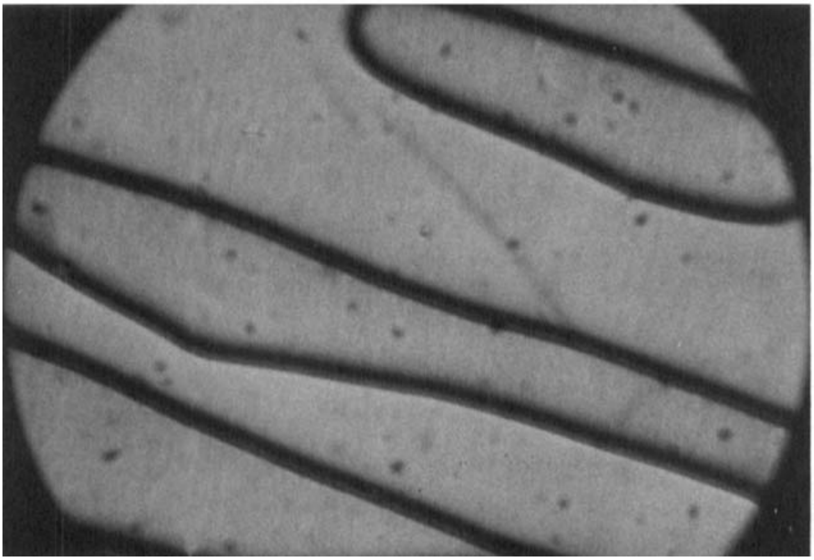

(d)

See color figures at end of issue.

Although the light scattering profile from periodic lines shows diffraction pattern, the direction of helical axis is controlled by rubbing direction. Therefore, diffraction pattern appears in one direction (Figure 4b).

In the neighborhood of the threshold field, the periodic lines remarkably disappear in part to form some color regions (Figure 3d). The light scattering pattern from this state has its maximum in one direction (Figure 4c). We have calculated the relation between the direction of molecular axis and its scattering pattern on the basis of Rhodes's approach.[7]

Figure 4d shows the coordinate system used to relate the scattered beam to a rod representing liquid crystal molecule. The direction of a rod, the maximum polarizability direction, is expressed by the angle α and ϕ.

The two angles which define the unit vector S' in the direction of the scattered radiation are the angle θ between the scattered beam and the incident beam (S_0) along x-axis, and the angle Ω which lies in the yz-plane. The incident beam and the scattered beam are polarized in the vertical (V) or horizontal (H) direction. The origin of the coordinate system is located at the center of the rod.

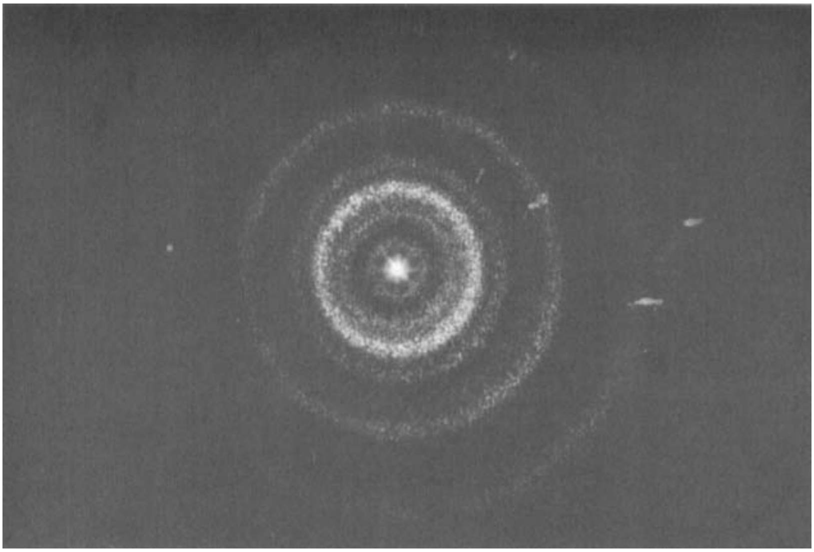

(a)

FIGURE 4 Photographs of the light scattering characteristic of the sample under an electric field: $d/p = 2.20$: using He—Ne laser ($\lambda = 632.8$ nm). (a) Diffraction pattern from homeotropic boundary condition sample: $E = 112$ V/mm; (b) Diffraction pattern from parallel boundary condition sample: $E = 255$ V/mm; (c) Scattering pattern from sample (b): $E = 292$ V/mm; (d) Coordinate system for rod scattering calculation; (e) Theoretical contour of (c) state: in the case of parallel polarizers.

(c)

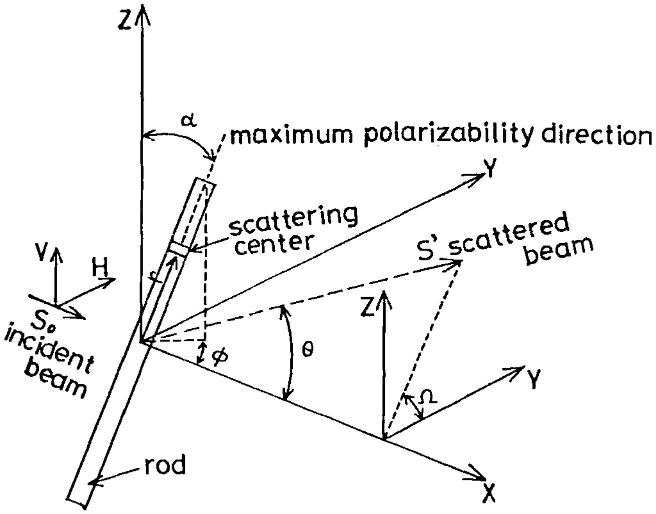
Z
α
maximum polarizability direction
Y
scattering center
S' scattered beam
V
H
S₀ incident beam
Z
φ
θ
Ω
Y
rod
X

(d)

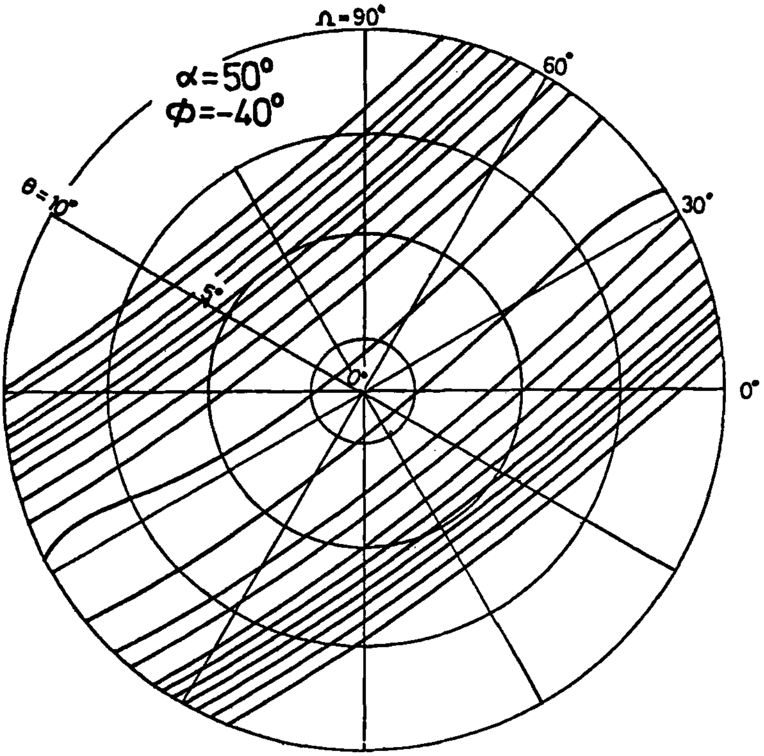
Ω=90°
60°
30°
0°
α=50°
Φ=-40°
θ=10°
5°
0°

(e)

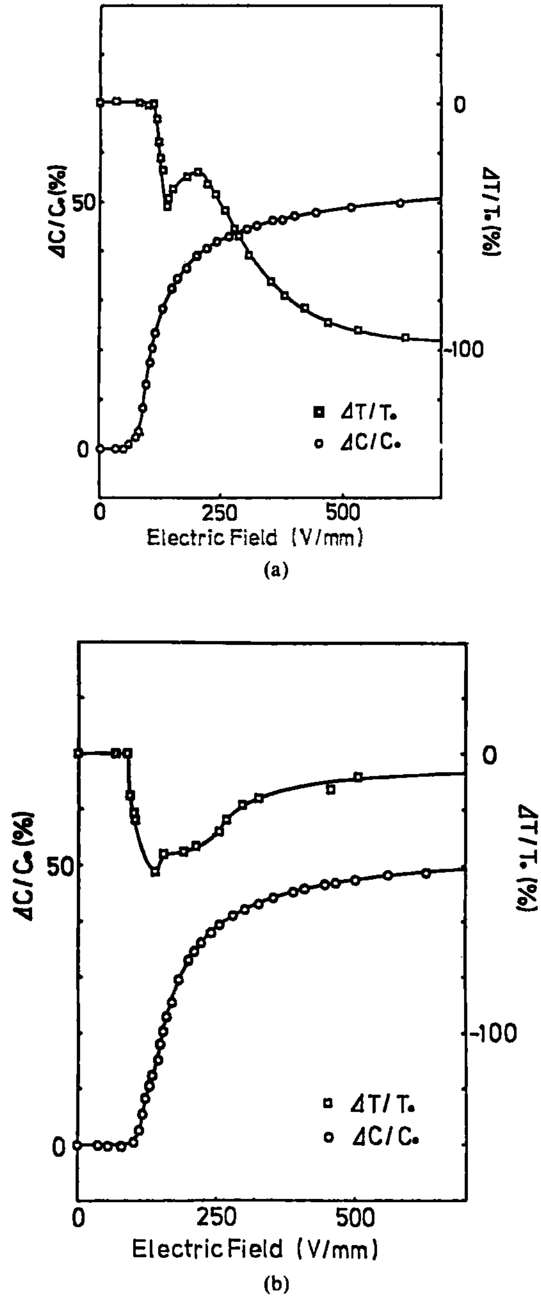

FIGURE 5 Relative capacitance change and relative transmission change vs. applied electric field: parallel boundary condition sample was used. (a) $d/p = 0.25$: crossed polarizers; (b) $d/p = 0.75$: without polarizers.

The procedure of calculation[7] is that the amplitude of the scattered radiation originating from a single scattering center is summed over all scattering centers and squared to obtain the intensity of the scattered radiation. Supposing that the structures already change into nematic state in the color regions, we made the distribution function of rods constant.

When α has been chosen as 50° and ϕ as −40°, the calculated pattern has given good agreement with the pattern obtained in the experiment, as shown in Figure 4e. The results indicate that the molecules are tilted along the helical axis under the influence of surface treatment.

Figure 5 shows $\Delta C/C_0$ and $\Delta T/T_0$ in parallel boundary condition samples. From the viewpoint of the tilt angle, the characteristic in Figure 5 is remarkably different from the one of Figure 2.

Geometrical model of helical structure

The structures are influenced remarkably by d/p, by the treatment condition of plates, and by the applied field. Figure 6 shows some geometrical models of the helical structure with static deformation. Our examination of the data led to the selection of the azimuthal angle of a molecular layer ϕ and tilt angle in the direction of helical axis θ as the components of static deformation (Figure 6b). Therefore, we have defined a new parameter representing the degree of helical alignment as a function of ϕ and θ, which is to be shown in Sec. 4.

4 DEFINITION OF THE HELICAL ORDER PARAMETER

From the experiments mentioned above, we define the helical order parameter, so that it clarifies the degree of the helical alignment. The system is assumed to be monodomain cholesteric phase whose layers have nematic orientation and are twisted continuously along the helical axis, provided that local deformation and defects are neglected.

$$Q \equiv 2\{1 - [\langle \sin^2 \phi \rangle]\} \cdot [\langle \cos^2 \theta \rangle] \equiv 2(1 - r) \cdot q \tag{1}$$

where ϕ is the azimuthal angle of a molecular, θ is the tilt angle in the direction of helical axis, $\langle \quad \rangle$ denotes an average over time, and $[\quad]$ denotes a spacial average over a half-pitch; i.e.

$$[F] = \frac{\int_0^{p/2} F \, dz}{\int_0^{p/2} dz}$$

where z is the position on the helical axis.

As shown in de Gennes's model,[5] it is reasonable to introduce ϕ in order to

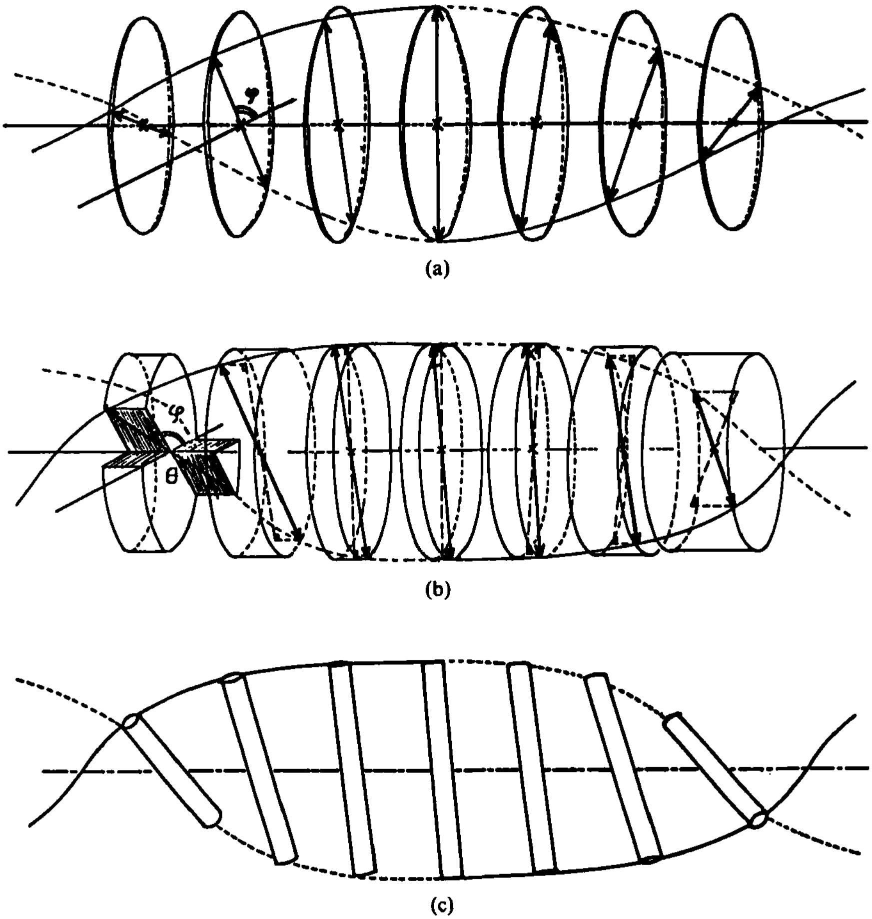

FIGURE 6 Geometrical arrangements of the helical structure. (a) The case of perfect alignment; (b) Static deformation: this model was drawn from the deformation for parallel boundary condition sample; (c) Schematic model: the direction of molecular rods in each layer (b).

represent a deformation of helical structure. θ is introduced when we think the results of experiments.

For the perfectly helical alignment,

$$\phi = \frac{2\pi z}{p}, \quad \theta = 0,$$

then $r = \frac{1}{2}$, $q = 1$, so that $Q = 1$.

For nematic state with helical structure disappearing, the relation $Q = 0$ holds. Especially, when the helical axis unwound by applied field and then the molecules get aligned normal to the helical axis (cholesteric-nematic phase change),

$$q = 1, \quad r = 1.$$

If twisted nematic state is also recognized as helical structure and electric field is applied parallel to the helical axis, the molecules get aligned parallel to the helical axis (twisted nematic—homeotropic nematic structure change),

$$q = 0, \quad r = 0.$$

Hence, Q varies from 1 to 0 according to the type and the degree of deformations.

Description of tensor property

We related Q with experimentally determinable quantities, i.e. the molecular tensor property, so that we can determine the value of Q. The coordinate systems for tensor property are defined as shown in Figure 7.

Let T'_{ij} be a component of microscopic tensor property of a nematic layer in the cholesterics, where i, j $(= \xi, \eta, \zeta)$ refer to Cartesian axes fixed in the nematic system of each layer and ζ axis is parallel to the director of the molecules of the layer.

Let T''_{mn} be the component of tensor in m, n frame, where m, n $(= \alpha, \beta, \gamma)$ refer to Cartesian axes fixed in the layer; β axis is parallel to the helical axis (Figure 7a).

In the case that the molecules in the layer are tilted toward helical axis, i, j frame rotates by θ around ξ axis coincident with α axis. γ direction, which is the projection of the director on the plane normal to helical axis, gives the spacial azimuth of the layer. Since T'_{ij} are assumed to have uniaxial symmetry, $\langle T'_{\xi\xi}\rangle = \langle T'_{\eta\eta}\rangle$.

The transformation relating $\langle \mathbf{T}''\rangle$ to $\langle \mathbf{T}'\rangle$ is given by

$$\langle T''_{mn}\rangle = \sum_{i} \langle B_{mi}B_{ni}\rangle\langle T'_{ii}\rangle, \tag{2}$$

where $\mathbf{B}$ is the matrix of direction cosines giving the local orientation of i, j frame in m, n frame.

Let $T_{\mu\nu}$ be the component of a tensor in the cholesteric laboratory frame, where μ, ν $(= x, y, z)$ refer to space-fixed Cartesian axes and z axis is parallel to the helical axis. The m, n frame rotates in μ, ν frame along z axis by ϕ (Figure 7b). For the perfectly helical alignment, $d\phi/dz =$ const. (pitch $=$ const.); for nematic state, $d\phi/dz = 0$ (pitch is infinite).

The spacially averaged component of $\mathbf{T}$ is given by

$$[\langle T_{\mu\nu}\rangle] = \sum_{m,n} [\langle C_{\mu m}C_{\nu n}\rangle]\langle T''_{mn}\rangle, \tag{3}$$

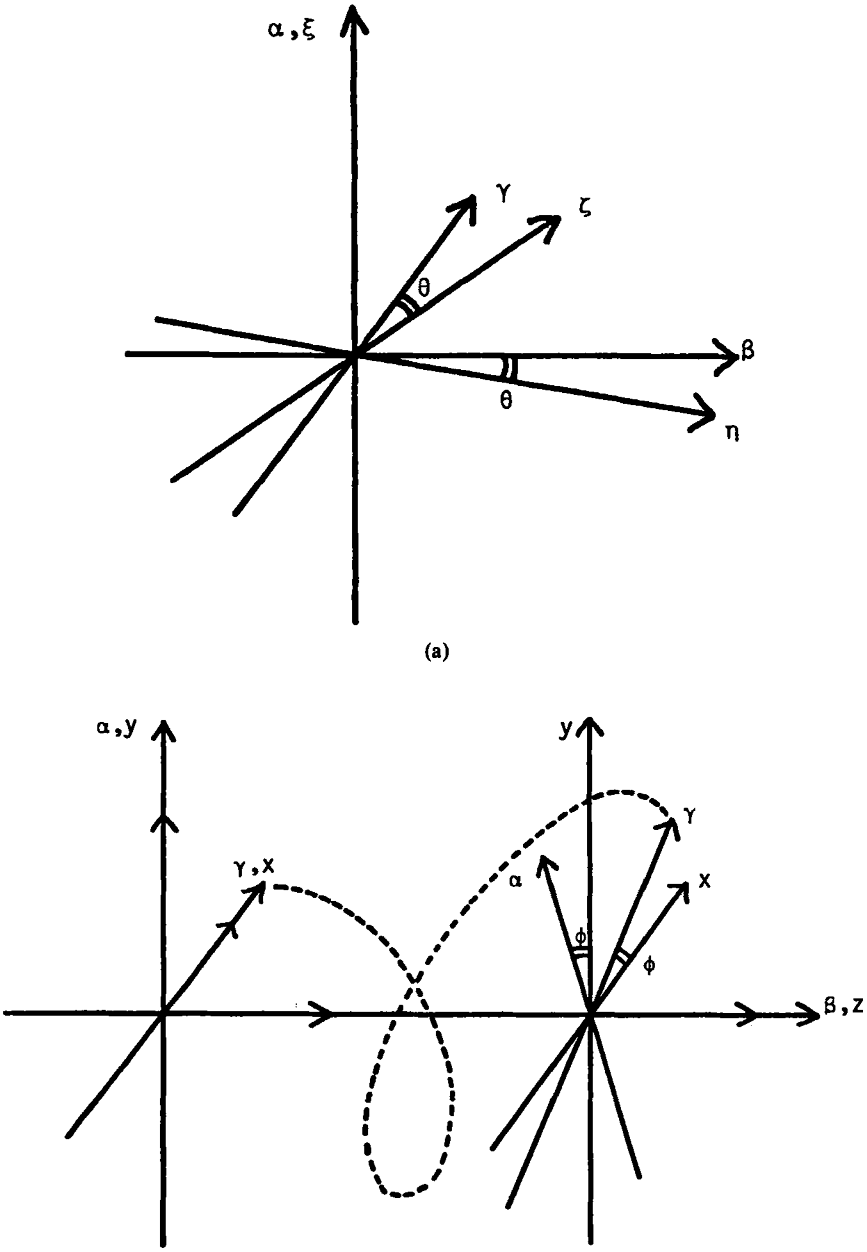

(a)

(b)

FIGURE 7 Coordinate systems for tensor property.

where **C** is the matrix of direction cosines.

Using Eqs. (2) and (3), the following results are obtained;

$$[\langle T_{xx}\rangle] = \langle T'_{\xi\xi}\rangle + \frac{1}{2}\, Q\, \langle \Delta T'\rangle \tag{4a}$$

$$[\langle T_{yy}\rangle] = \langle T'_{\xi\xi}\rangle + \left(q - \frac{1}{2}\, Q\right) \langle \Delta T'\rangle \tag{4b}$$

$$[\langle T_{zz}\rangle] = \langle T'_{\zeta\zeta}\rangle - q\, \langle \Delta T'\rangle \tag{4c}$$

$\langle \Delta T'\rangle$ is the uniaxial anisotropy given by

$$\langle \Delta T'\rangle = \langle T'_{\zeta\zeta}\rangle - \langle T'_{\xi\xi}\rangle. \tag{5}$$

Since both $\langle T_{\mu\mu}\rangle$ and $\langle T'_{ii}\rangle$ are experimentally determined quantities (such as dielectric constants, refractive indices and susceptibilities), Q can be derived from them.

Typical descriptions of tensor components are as follows; for perfectly helical alignment,

$$[\langle T_{xx}\rangle] = \frac{1}{2}\{\langle T'_{\xi\xi}\rangle + \langle T'_{\zeta\zeta}\rangle\} = [\langle T_{yy}\rangle] \tag{6a}$$

$$[\langle T_{yy}\rangle] = \frac{1}{2}\{\langle T'_{\xi\xi}\rangle + \langle T'_{\zeta\zeta}\rangle\} = [\langle T_{xx}\rangle] \tag{6b}$$

$$[\langle T_{zz}\rangle] = \langle T'_{\xi\xi}\rangle = \langle T'_{\eta\eta}\rangle \tag{6c}$$

for cholesteric-nematic phase change,

$$[\langle T_{xx}\rangle] = \langle T'_{\xi\xi}\rangle = \langle T'_{\eta\eta}\rangle \tag{7a}$$

$$[\langle T_{yy}\rangle] = \langle T'_{\zeta\zeta}\rangle \tag{7b}$$

$$[\langle T_{zz}\rangle] = \langle T'_{\xi\xi}\rangle = \langle T'_{\eta\eta}\rangle \tag{7c}$$

and for twisted nematic to homeotropic nematic structure change,

$$[\langle T_{xx}\rangle] = \langle T'_{\xi\xi}\rangle = \langle T'_{\eta\eta}\rangle \tag{8a}$$

$$[\langle T_{yy}\rangle] = \langle T'_{\xi\xi}\rangle = \langle T'_{\eta\eta}\rangle \tag{8b}$$

$$[\langle T_{zz}\rangle] = \langle T'_{\zeta\zeta}\rangle \tag{8c}$$

5 DISCUSSION

Comparison with de Genne's model

De Gennes's calculation is known as the analysis of field-induced cholesteric-nematic phase change.[5] In the calculation, applied magnetic field is normal to helical axis and the structure deformation is assumed to be represented by only ϕ. The critical field strength of phase change H_{th}, pitch length and azimuthal angle are given by

$$H_{th} = \left(\frac{\pi}{2}\right) q_0 \left(\frac{k_{22}}{\chi_a}\right)^{1/2},$$

$$p = \left(\frac{4}{\pi}\right) K_{(k)} E_{(k)} p_0,$$

$$\phi = \arcsin\left[\mathrm{sn}(\pi^2/E_{(k)} p_0 \cdot z \,|\, k)\right],$$

where k_{22} is the twist elastic constant, χ_a is diamagnetic anisotropy, $K_{(k)}$ and $E_{(k)}$ are the complete elliptic integrals of first and second kind, respectively, and q_0 is the initial pitch wave vector.

We evaluated Q values compare with this model as shown in Figure 8. The curves for the samples in homeotropic boundary condition agree with the theoretical curve of Q_t. Especially, the curve obtained from the sample of $d/p = 1.18$, in which the static deformation characteristic mainly lies in azimuthal angle change of molecular layer (Figure 1a–d), is in good agreement with the theoretical curve of Q_t. As d/p increases, Q_e curve gets away from Q_t curve. On the other hand, the curve for parallel boundary condition sample is quite different from Q_t.

As shown above, the deviation from Q_t curve originates from the reason that in de Gennes's model the deformation is assumed to be represented by ϕ

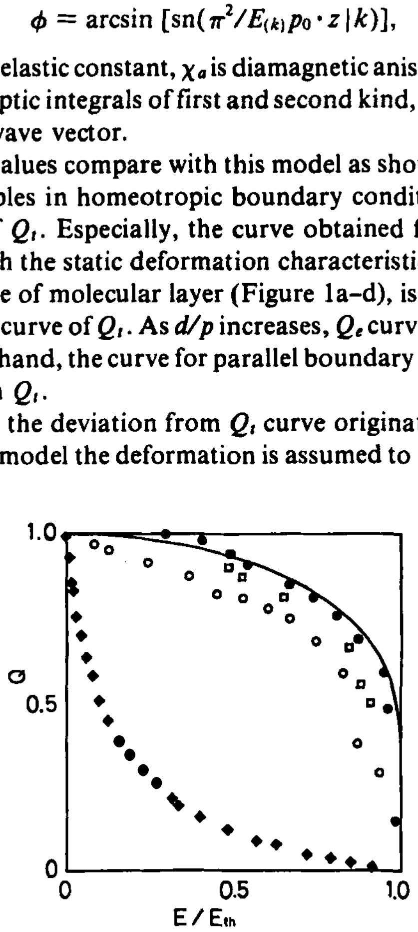

FIGURE 8 Dependence of Q values on the normalized electric field strength: E_{th} is the critical field of cholesteric-nematic phase change. Solid line (Q_t): theoretical Q value ($q = 1$) predicted in de Gennes's model. Plots (Q_e): helical order parameter Q obtained with relative capacitance (for the purpose of comparing with de Gennes's model, Q_e is adjusted to the condition that $q = 1$ (see APPENDIX).). ●□○: homeotropic boundary condition samples; d/p—● 1.18; □ 1.52; ○ 3.38. ■: parallel boundary condition sample; $d/p = 0.75$.

only. However, in the actual structure the deformation should be represented by ϕ and θ, and $q \neq 1$ in general. If q is modified according to deformation, Q_t curve fits well to each data. Therefore the expression of Q including r and q is proved to be more available for evaluating the deformation. De Gennes's model can be applied to determine the pitch change and the critical field, but not to express the actual deformation.

Relation to the nematic order parameter

Recently there were studies[3,4] to measure the orientational order in cholesteric phase using the nematic order parameter S, which is introduced by Maier and Saupe.[1,2] Here we discuss the relationship between Q and S. In order to show this, following tensors are needed.

Let T'''_{kl} be a component of the tensor property of a molecule, and $k, l (= 1, 2, 3)$ refer to Cartesian coordinate system fixed to a molecule. Let T^0_{ij} be a component of a microscopic tensor of a nematic system and $i, j (= \xi, \eta, \zeta)$ are Cartesian coordinate in a laboratory frame where ζ axis is parallel to the director.

Then,

$$\langle T^0_{ij} \rangle = \sum_{k,l} \langle A_{ik} A_{jl} \rangle \langle T'''_{kl} \rangle, \tag{9}$$

where A_{ik} is the matrix of direction cosines. The uniaxial symmetry of nematic phase being considered, $\langle \mathbf{T}^0 \rangle$ becomes diagonal. Then, $\langle T^0_{\xi\xi} \rangle = \langle T^0_{\eta\eta} \rangle$, and the uniaxial anisotropy is given by[3]

$$\begin{aligned} \langle \Delta T^0 \rangle &\equiv \langle T^0_{\zeta\zeta} \rangle - \langle T^0_{\xi\xi} \rangle \\ &= \frac{3}{2} \sum_{k,l} \langle A_{\zeta k} A_{\zeta l} \rangle \langle T'''_{kl} \rangle, - \frac{1}{2}\, tr\, \langle T''' \rangle. \end{aligned} \tag{10}$$

The nematic order parameter S_{kl} was defined by

$$S_{kl} = \frac{1}{2} \langle 3 A_{\zeta k} A_{\zeta l} - \delta_{kl} \rangle, \tag{11}$$

where δ_{kl} is Krönecker delta. Accordingly,

$$\langle \Delta T^0 \rangle = \sum_{k,l} S_{kl} \langle T'''_{kl} \rangle. \tag{12}$$

In the case of cholesteric phase, the uniaxial symmetry is lost because of the existance of helical axis and biaxiality appears. But the order of $(q_0 a)^2$ (q_0; pitch wave vector, a; a molecular length) is very small ($\simeq 10^{-4}$), so that it doesn't contribute to the energy per unit volume associated with the nematic order. Then, $\langle \Delta T^0 \rangle \simeq \langle \Delta T' \rangle$.

In Eqs. (4) and (12), $\langle T_{\mu\mu}\rangle$, $\langle T_{ii}\rangle$ and $\langle T''_{kl}\rangle$ are experimentally determinable quantities, and Q can be derived from Eq. (4), as mentioned above, so there is the possibility to measure S with Q.

6 CONCLUSION

We have investigated the helical structures with static deformation by several experiments and proposed the "helical order parameter" Q, which shows the helical properties of cholesteric phase numerically on the basis of nematic phase. As Q is a experimentally determined quantity using a second order tensor property, the type and the degree of deformation in the helical structure are expressed by the one value. Furthermore we have given examples of Q, and discussed the relationship between Q and the nematic order parameter. We also evaluated the utility of Q.

References

1. W. Maier and A. Saupe, *Z. Naturforsch.*, **13a**, 564 (1958); *Z. Naturforsch.*, **14a**, 882 (1959); *Z. Naturforsch.*, **15a**, 287 (1960).
2. A. Saupe, *Z. Naturforsch.*, **19a**, 161 (1964).
3. P. J. Collings, S. I. Goss and J. R. McColl, *Phys. Rev. A*, **11**, 684 (1975).
4. E. H. Korte, *Mol. Cryst. Liq. Cryst.*, **44**, 151 (1978).
5. P. G. deGennes, *Sol. State Commun.*, **6**, 163 (1968).
6. R. B. Meyer, *Appl. Phys. Letters*, **12**, 281 (1968); *Appl. Phys. Letters*, **14**, 208 (1969).
7. M. B. Rhodes and R. S. Stein, *J. Polym. Sci. A-2*, **7**, 1539 (1969).

Appendix

When y-axis is parallel to the applied field and z-axis is along to the helical axis, the dielectric constant of the molecules of a layer is

$$\epsilon_\phi = \epsilon_\perp\langle\cos^2\phi\rangle + \epsilon_\parallel\langle\sin^2\phi\rangle \qquad \text{(A1)}$$

where $\epsilon_\perp$ and $\epsilon_\parallel$ are the respective dielectric constants for the long axis of molecule aligned normal and parallel to the applied field, and ϕ is the angle between the director of the molecular layer and x-axis.

The average dielectric constant in the y-direction, $\tilde{\epsilon}_y$, is given by averaging ϵ_ϕ.

$$\begin{aligned}\tilde{\epsilon}_y &= \frac{2}{p}\int_0^{p/2}\epsilon_\phi dz\\ &= \epsilon_\perp + (\epsilon_\parallel - \epsilon_\perp)r \qquad (r = [\langle\sin^2\phi\rangle]) \qquad \text{(A2)}\end{aligned}$$

We define a relative capacitance C_R,

$$C_R = \frac{\tilde{\epsilon}_y - \dfrac{\epsilon_\parallel + \epsilon_\perp}{2}}{\epsilon_\parallel - \dfrac{\epsilon_\parallel + \epsilon_\perp}{2}} = 2r - 1 \tag{A3}$$

where $(\epsilon_\parallel + \epsilon_\perp)/2$ is the dielectric constant at zero field and $\epsilon_\parallel$ is at nematic phase (after a phase change).

In de Gennes's model, the structure deformation is assumed to be represented by only ϕ. So this means $\theta = 0$, and $q = 1$. When $q = 1$, Eq. (1) is

$$Q = 2(1 - r) \tag{A4}$$

And, from Eqs. (A3) and (A4),

$$C_R = 1 - Q \tag{A5}$$

Then we can obtain Q_e experimentally.

Using de Gennes's results,[5] Eq. (A2) is

$$\tilde{\epsilon}_y = \epsilon_\perp + \frac{\epsilon_\parallel - \epsilon_\perp}{2}\left\{1 - \frac{E(k)}{K(k)}\right\} \tag{A6}$$

From Eqs. (A3) and (A6), we obtain

$$C_R = \frac{2}{k^2}\left\{1 - \frac{E(k)}{K(k)}\right\} \tag{A7}$$

Therefore we can calculate Q_t using Eqs. (A5) and (A7).